Supplementary Information

Covalent organic framework isomers with discrepant photocatalytic properties

Xitong Ren,[a] Mengyao Wen,[a] Xiaobin Hou,[a] Jiajie Sun,[b] Feng Bai[a,*] and Yusen Li[a,*]

[a] Key Laboratory for Special Functional Materials of Ministry of Education, National and Local Joint Engineering Research Center for High-Efficiency Display and Lighting Technology, School of Materials Science and Engineering, and Collaborative Innovation Center of Nano Functional Materials and Applications, Henan University, Kaifeng 475004, China.

[b] School of Physics and Electronics, Henan University, Kaifeng 475004, China.

Experimental Details

Characterizations. Powder X-ray diffraction (PXRD) patterns of afforded isomeric COFs were recorded on a D8 ADVANCE X-ray diffractometer with Cu Kα radiation (λ = 0.15406 nm). The porous structure was investigated by N_2 adsorption/desorption at liquid nitrogen temperature (BELSORP, MicrotracBEL) and the samples were degassed at 120 °C for 8 h before measurement. Ultraviolet-visible spectroscopy diffuse reflectance spectra (Uv-vis DRS) were obtained by a UV-vis spectrophotometer (Agilent Cary 5000). The sample morphology was characterized by field emission scanning electron microscope (JSM-7900F, AztecLive UltimMax 40) and transmission electron microscope (JEOL JEM-F200 and JEOL JEM-2100). Electron paramagnetic resonance (EPR) was measured on a Bruker EMXplus-6/1 spectrometer at room temperature. The orbital analysis was performed by density functional theory (DTF) calculation, energy task with fine quality, and available Eigenvalues of HOMO and LUMO were generated after the task successfully terminated.

Photoelectrochemical Measurements. A series of electrochemical workstations (Autolab PGSTAT302N, CHI760E, and PEC2000 photoelectric chemical test system, Perfect Light) were used to proceed with the photoelectrochemical measurements, including the photocurrent tests, electrochemical impedance spectra (EIS), and Mott-Schottky plot. Photocurrent tests were executed in a conventional three-electrode system with a Pt foil as the counter electrode and an Ag/AgCl electrode as the reference electrode, and a PLS-FX300HU lamp (100 mW/cm^2) was employed as the optical source. COF powders (1 mg) and Nafion (5 μL, 5 wt%) were dispersed in the mixture of water/ethanol (200 μL, 1:1 v/v), and sonicated for at least 20 min to form a homogeneous ink. The working electrode was prepared by drop-casting the obtained ink (100 μL) onto FTO glass with an area of 1 cm^2. And the working electrodes were prepared by drop-casting the above ink (5 μL) onto GCE with diameter of 3 mm, Na_2SO_4 solution (0.2 M, pH = 7) was used as the electrolyte. As to the Mott-Schottky plot was collected at the same system. The applied potentials vs. Ag/AgCl were

converted to NHE potentials using the following equation[1]:

$$E_{RHE} = E_{(Ag/AgCl)} + 0.0591pH + E^{\theta}_{(Ag/AgCl)}$$

$$E_{NHE} = E(Ag/AgCl) + E^{\theta}(Ag/AgCl)\ (E^{\theta}(Ag/AgCl) = 0.199\ V)$$

Photocatalytic activity evaluation. A 300 mL closed quartz flask reactor with a top-irradiation model was utilized to proceed with photocatalytic H_2 production reactions, which was sealed with seal rubber septa (Beijing China Education Au-Light). Typically, 10 mg of the prepared COF powder was dispersed in 100 mL aqueous solution (DMF: water = 1:9, V : V) with 0.2 M AA as the sacrificial agent and 5 wt.% Pt as cocatalyst which was in situ photo-deposited on the surface of the photocatalysts using K_2PtCl_6 as the precursor.[S1] The system was vacuumed for 30 min, then the solution was irradiated by a 300 W Xenon lamp with a UV-cutoff filter ($\lambda > 420$ nm) under continuous stirring and the reaction temperature was kept steadily at 4°C. The hydrogen evolution was detected using an online gas chromatograph (GC-7920) equipped with a thermal conductivity detector (TCD), the carrier gas was nitrogen.

Experimental procedure of photodegradation of RhB: Obtained COFs (25 mg) were dispersed into the solution of rhodamine B (25 mg L^{-1}), then magnetically stirred for 30 min in the dark. After this, the mixture was allowed to be exposed to visible light ($\lambda >$ 420 nm) from a 300 W Xenon lamp at a distance of ~5 cm between the liquid surface and the lamp. The solution was kept stirring during irradiation. At an interval of 10 min, 4 mL of the mixture was taken out of the beaker for analysis after centrifugation

Materials. All the chemicals and reagents are commercially available from Adams, Aldrich, J&K Scientific, TCI chemicals and are used without further purification. 1,3,6,8-tetrakis(4-formylphenyl)pyrene (Py-4CHO), 1,3,6,8-tetrakis(4-aminophenyl)pyrene (Py-4NH_2) and 4,7-Diaminobenzo[c][1,2,5]thiadiazole (BT-2NH_2) were synthesized according to literature methods.

Synthesis of 4,7-Diaminobenzo[c][1,2,5]thiadiazole (BT-2NH_2).[S2] To a solution of 4-aminobenzo[c][1,2,5]thiadiazole (5.0 g, 33.1 mmol) in 0.6 mol/L HCl (100 mL) was added portionwise at 0 °C p-benzenediazonium sulfonate. Preapared from sulfanilic acid (7.85 g, 45.4 mmol)/water (37.5 mL) and $NaNO_2$ (3.3 g,47.5 mmol)/water(22.5 mL) under 15 min strring. After stirring for 2.5 h at 0 °C, dark reddish precipitates of the azo dye were filtered and washed with water and acetone. After drying in vacuo, the well-ground powder was suspended in 3 mol/L NaOH(aq) (150 mL). To this solution was added portion-wise $Na_2S_2O_4$ (12.5 g, 144 mmol) at 50 °C, and the mixture was heated at 90 °C for 2 h. After cooling, the mixture was extracted with dichloromethane. The organic layer was washed with saturated aqueous $NaHCO_3$.The crude product was purified by column chromatography to afford a deep-red solid Recrystallization from MeOH gave reddish needles. And the final product 4,7-Diaminobenzo[c][1,2,5]thiadiazole was dried under vacuum. (2.0 g, 36.3%).^{1}H-NMR: (500 MHz, $CDCl_3$: *ppm*) 6.53 (s, 2H, Ar-H), 4.15 (s, 4H, NH_2).

Synthesis of Py-*C*-BT-COF. Py-4CHO (6.2 mg, 10 μmol) and BT-2NH_2 (3.3 mg,20 μmol) were added to a 10 mL Schlenk tube, mesitylene (0.9 mL) and BnOH (0.1 mL) were added. The mixture was sonicated for 5 minutes followed by the addition of 3 M acetic acid (0.1 mL). The mixture was further sonicated for another 5 minutes and degassed by three freeze–pump–thaw cycles, purged with Ar, and heated at 120 °C for 3 days. Upon cooling to r.t., the precipitate was collected by filtration and washed by DMF, methanol DCM, dried under vacuum to afford a brown powder (7.5 mg, 78%). Elemental analysis (wt.%) calcd. For $\{C_{58}H_{36}N_6S_2\}_n$: C 79.07, H 4.12, N 9.54, S 7.28; found: C 81.1, H 4.70, N 9.28, S 4.90.

Synthesis of Py-*N*-BT-COF. Py-4NH_2(5.7 mg, 10 μmol) and BT-2CHO (3.9 mg, 20 μmol) were added to a 10 mL Schlenk tube, and mesitylene (0.2 mL) and BnOH (0.8 mL) were added. The mixture was sonicated for 5 minutes followed by addition of 6 M acetic acid (0.1 mL). The mixture was further sonicated for another 5 minutes and degassed by three freeze–pump–thaw cycles, purged with Ar, and heated at 120 °C for

3 days. Upon cooling to r.t., the precipitate was collected by filtration and washed by DMF, methanol DCM, dried under vacuum to afford a crimson powder (8.5 mg, 89%). Elemental analysis (wt.%) calcd. For $\{C_{58}H_{36}N_6S_2\}_n$: C 79.07, H 4.12, N 9.54, S 7.28; found: C 78.16, H 4.18, N 11.65, S 6.01.

Structural Characterization

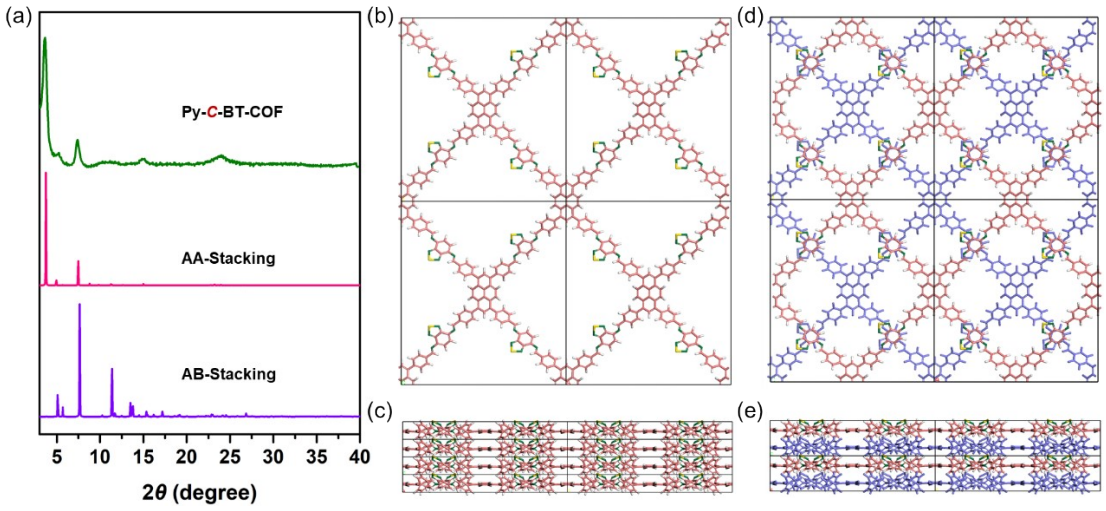

Figure S1. (a) Experimental PXRD patterns of Py-*C*-BT-COF (green), simulated profiles of AA-stacking model (pink) and AB-stacking model (violet); (b) and (c) Top and side view of Py-*C*-BT-COF in AA-stacking model; (d) and (e) Top and side view of Py-*C*-BT-COF in AB-stacking model.

Table S1 Atomic coordinates of the AA-stacking model of Py-*C*-BT-COF using DFTB method.

Space group: *C*M ***a* = 34.2384 Å, *b* = 34.5346 Å, *c* = 3.7859 Å.** ***α* = *γ* = 90°, and *β* = 65.1219°**			
	X	**Y**	**Z**
C1	0.96758	4.08246	0.46796
C2	0.96818	4.04134	0.44879
C3	1.00409	4.02069	0.45279
C4	1.03999	4.04133	0.45717
C5	1.04075	4.08244	0.43559
C6	1.00422	4.1021	0.45063
C7	1.07314	3.98023	0.50284
C8	0.93478	4.01977	0.40694
C9	0.92908	4.10518	0.51417
C10	1.07921	4.10504	0.39213
C11	0.93307	4.13888	0.30636
C12	0.89712	4.16102	0.35735
C13	0.85229	4.11781	0.83747

C14	0.88813	4.09515	0.78093
C15	1.12038	4.09446	0.13232
C16	1.15635	4.11658	0.083
C17	1.11113	4.1607	0.55256
C18	1.07512	4.13896	0.59736
N19	0.82194	3.79744	0.45329
C20	0.81837	3.82562	0.67602
C21	0.8561	3.84901	0.62349
C22	1.15243	3.85018	0.29633
N23	1.18633	4.20147	0.46692
C24	1.19029	4.17259	0.25121
C25	1.2964	3.24019	0.27989
C26	1.28726	3.27518	0.47164
C27	1.24247	3.28622	0.66094
C28	1.20914	3.26053	0.64856
C29	1.22052	3.22448	0.44864
C30	1.2641	3.21522	0.27131
N31	1.22872	3.31868	0.84952
S32	1.17001	3.31829	1.03471
N33	1.1687	3.27202	0.82652
H34	1.00428	4.13396	0.44935
H35	1.09823	3.96425	0.5484
H36	0.90948	4.03576	0.36472
H37	0.96487	4.14705	0.09794
H38	0.90033	4.18693	0.19115
H39	0.82068	4.10991	1.0504
H40	0.8848	4.06981	0.95436
H41	1.12387	4.06909	-0.04106
H42	1.1882	4.10825	-0.12409
H43	1.10779	4.18684	0.7162
H44	1.04312	4.14761	0.79936
H45	0.78725	3.8329	0.9099
H46	1.2218	4.16404	0.02636
H47	1.33022	3.23155	0.13442
H48	1.27431	3.18793	0.11983

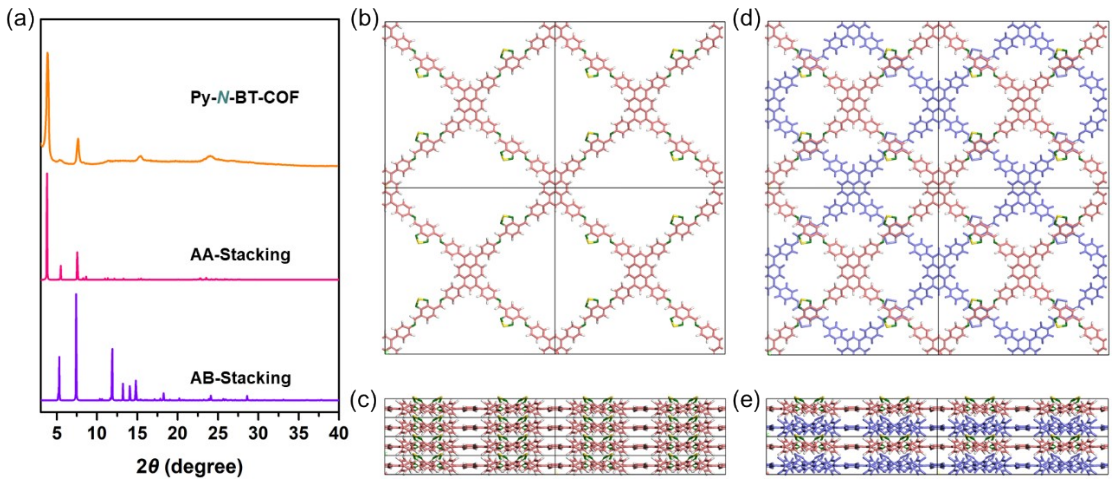

Figure S2. (a) Experimental PXRD patterns of Py-*N*-BT-COF (orange), simulated profiles of AA-stacking model (pink) and AB-stacking model (violet); (b) and (c) Top and side view of Py-*N*-BT-COF in AA-stacking model; (d) and (e) Top and side view of Py-*N*-BT-COF in AB-stacking model.

Table S2. Atomic coordinates of the AA-stacking model of Py-*N*-BT-COF using DFTB method.

Space group: *C*M **a = 35.5139 Å, b = 32.9271 Å, c = 3.7386 Å.** **$\alpha = \gamma$ = 90°, and β = 71.9230°**			
	X	**Y**	**Z**
C1	0.03691	0.04315	0.48119
C2	0.03685	0.0864	0.46425
C3	0.0692	0.02084	0.53048
C4	0.07281	0.1103	0.44787
C5	0.10901	0.09937	0.22284
C6	0.1427	0.12281	0.20173
C7	0.10447	0.16712	0.62591
C8	0.07094	0.14385	0.64243
C9	0.14096	0.15635	0.39963
C10	0.2854	0.23714	0.2774
C11	0.28764	0.27219	0.4409
C12	0.25172	0.28981	0.64637
C13	0.21393	0.27071	0.66317
C14	0.21306	0.23382	0.48785
C15	0.24907	0.21718	0.29869
N16	0.25063	0.31987	0.83968
S17	0.19878	0.327	1.07585
N18	0.18221	0.28597	0.87448

C19	0.17583	0.21193	0.51524
C20	0.32568	0.29163	0.41222
N21	0.17625	0.17834	0.36952
N22	0.32735	0.32323	0.56926
C23	0.00244	0.02175	0.46318
C24	0.00229	0.10714	0.46579
C25	0.46782	0.58635	0.46595
C26	0.46791	0.54314	0.4462
C27	0.43172	0.61004	0.48551
C28	0.43325	0.6439	0.29455
C29	0.39939	0.66678	0.31377
C30	0.36178	0.62147	0.73452
C31	0.39575	0.5984	0.71038
C32	0.36298	0.34474	0.53897
C33	0.93568	0.02084	0.39587
H34	0.0937	0.0374	0.57473
H35	0.11058	0.07319	0.06549
H36	0.17082	0.11385	0.02408
H37	0.10201	0.19347	0.78309
H38	0.04265	0.15266	0.81697
H39	0.31286	0.22255	0.12246
H40	0.24869	0.18869	0.16837
H41	0.14879	0.22773	0.66657
H42	0.35212	0.27597	0.24599
H43	0.00224	0.14059	0.46712
H44	0.46143	0.65324	0.12103
H45	0.40147	0.6935	0.15983
H46	0.33363	0.61216	0.9102
H47	0.39445	0.57212	0.86563
H48	0.9112	0.03739	0.35136

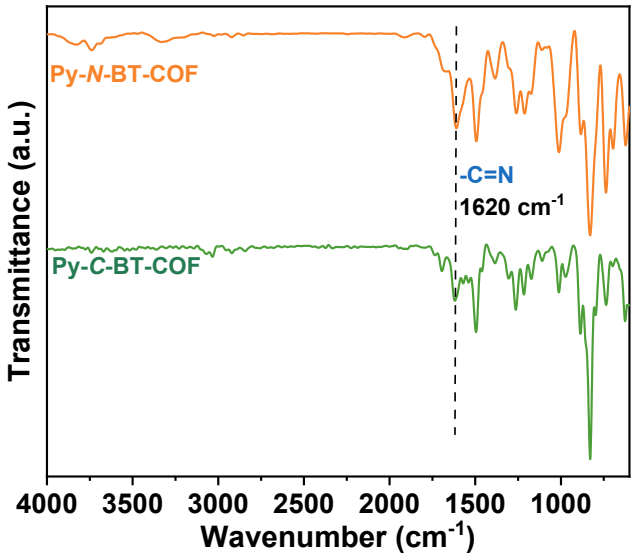

Figure S3. FT-IR spectra of Py-*C*-BT-COF (green) and Py-*N*-BT-COF (orange).

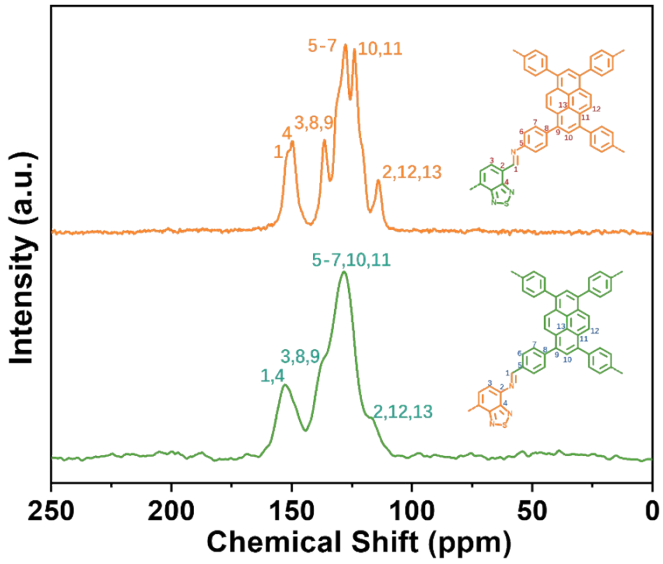

Figure S4. ^{13}C NMR spectra of Py-*C*-BT-COF (green) and Py-*N*-BT-COF (orange).

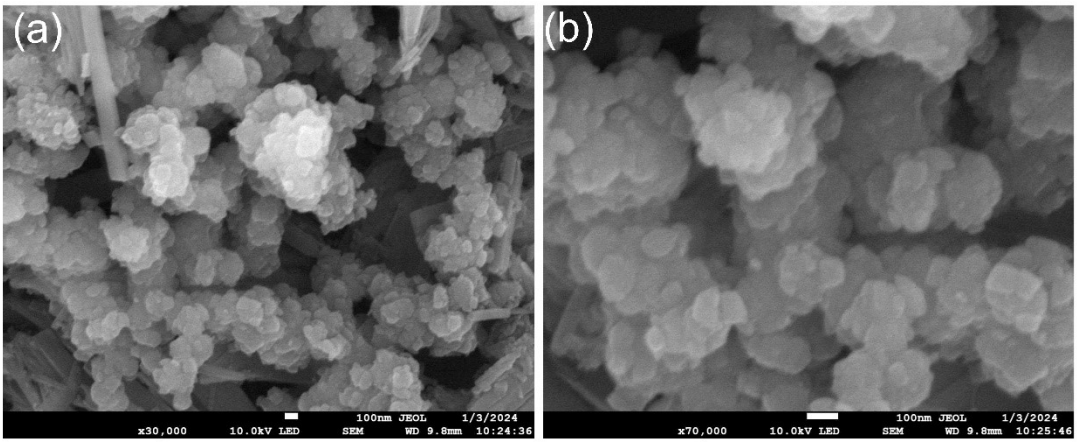

Figure S5. SEM images of Py-*C*-BT-COF.

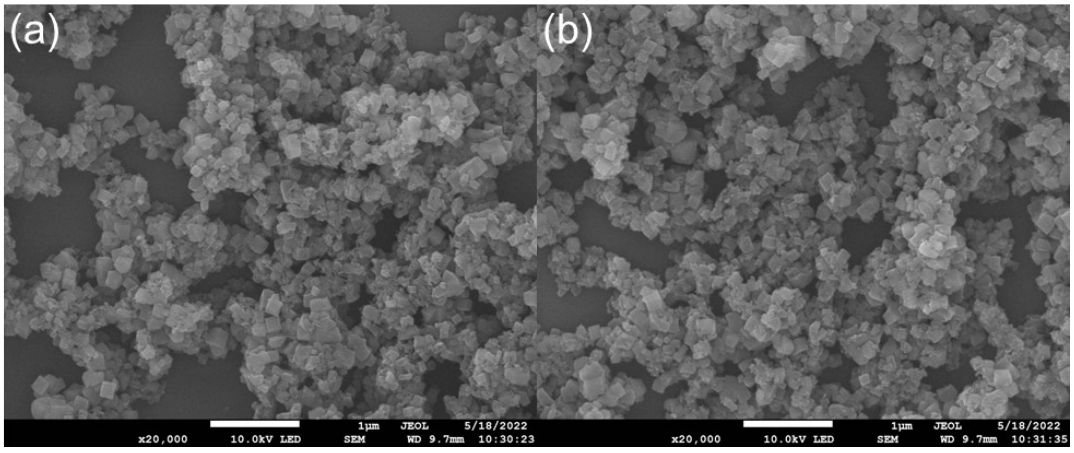

Figure S6. SEM images of Py-*N*-BT-COF.

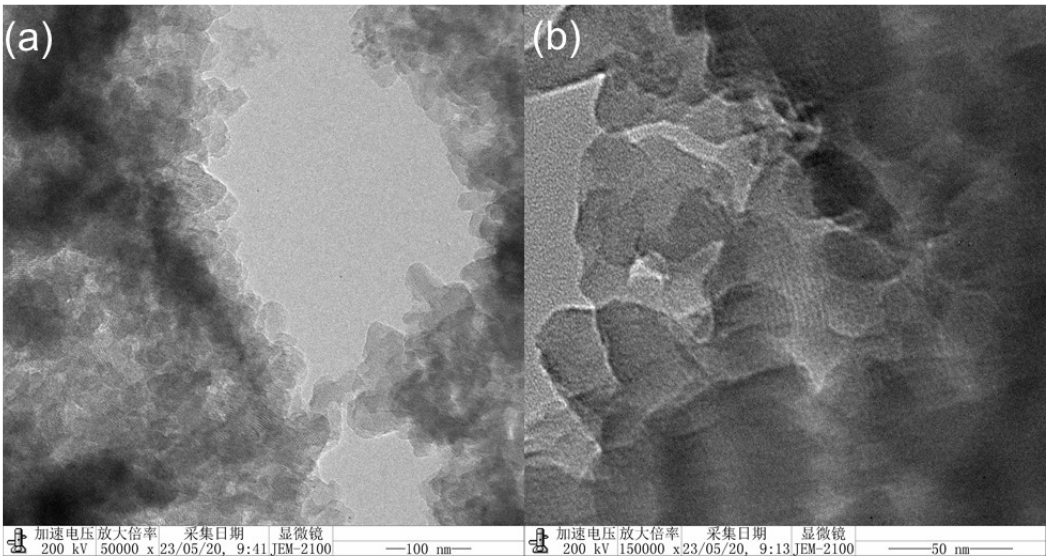

Figure S7. TEM images of Py-*C*-BT-COF.

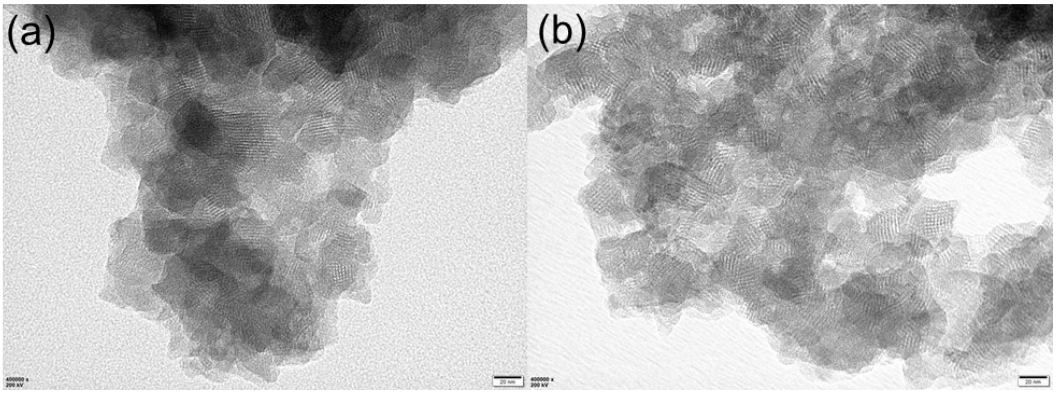

Figure S8. TEM images of Py-*N*-BT-COF.

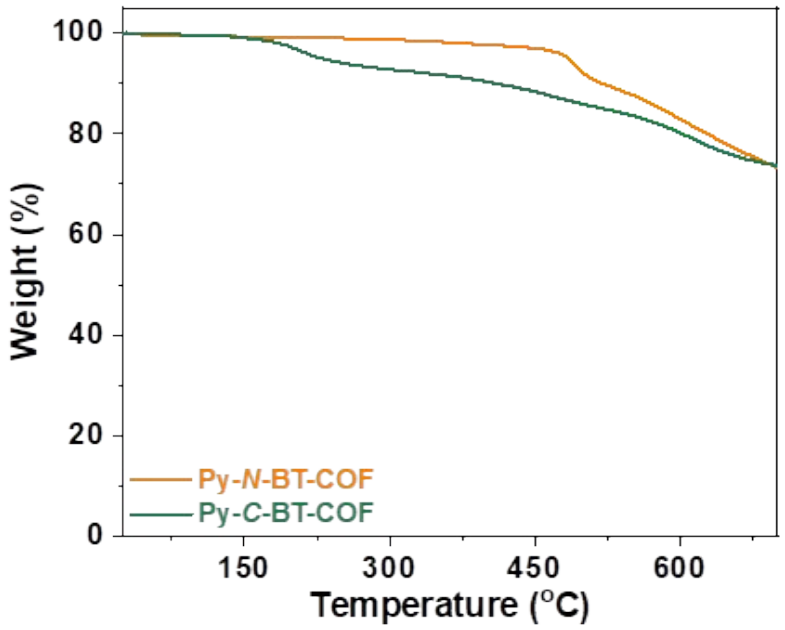

Figure S9. TGA profiles of Py-*C*-BT-COF and Py-*N*-BT-COF.

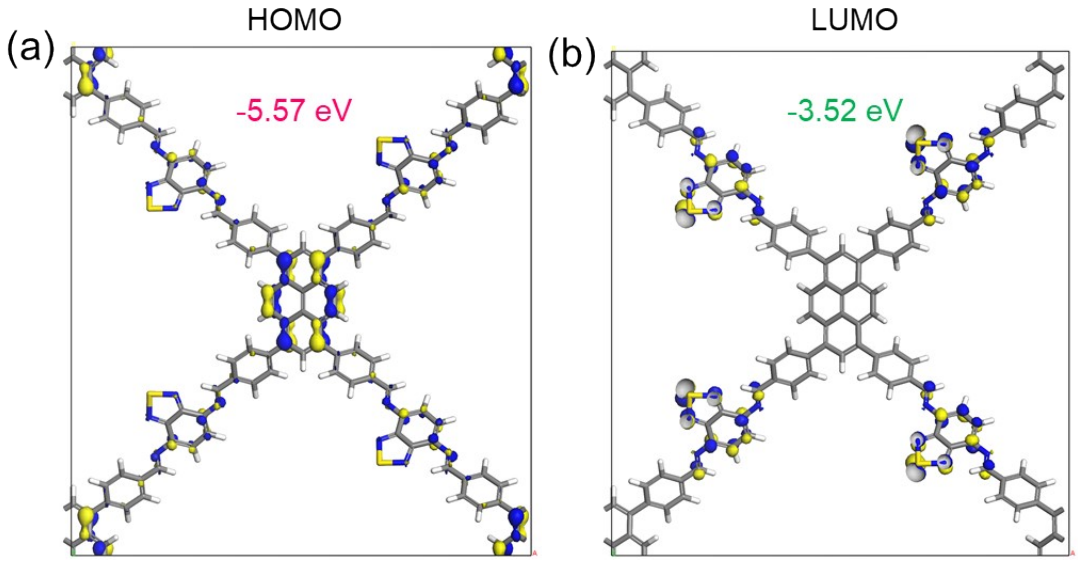

Figure S10. Calculated charge density distribution of HOMO and LUMO for Py-*C*-BT-COF, the band gap is afforded as 2.05 eV.

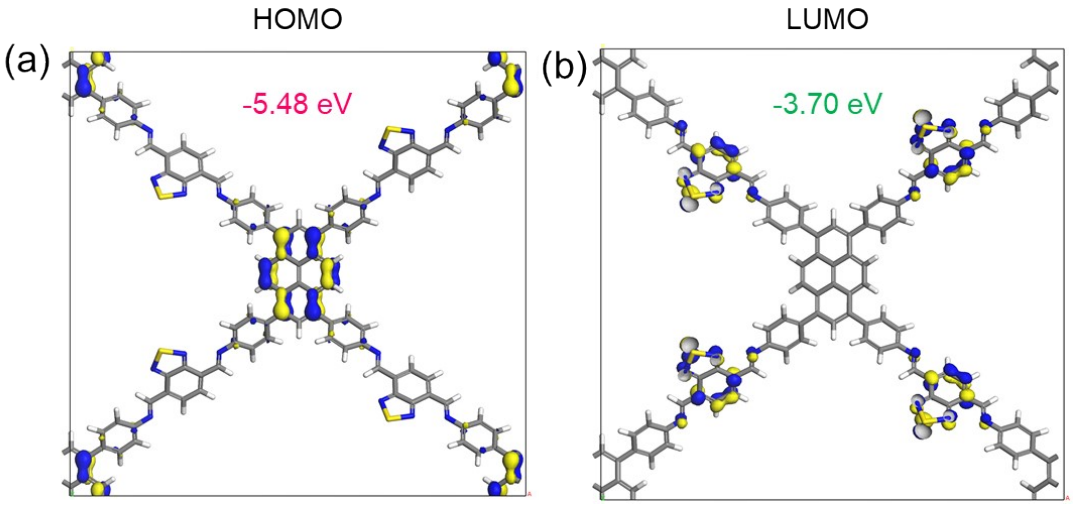

Figure S11. Calculated charge density distribution of HOMO and LUMO for Py-*N*-BT-COF, the band gap is afforded as 1.78 eV.

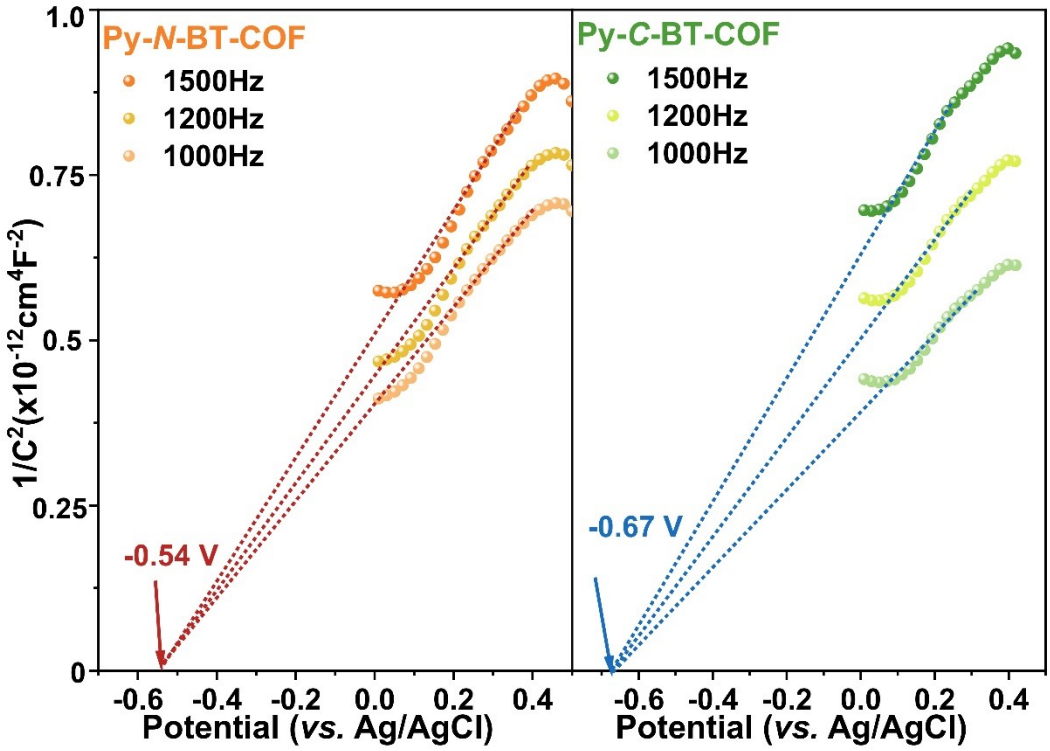

Figure S12. Mott-Schottky plots for Py-BT-COF isomers.

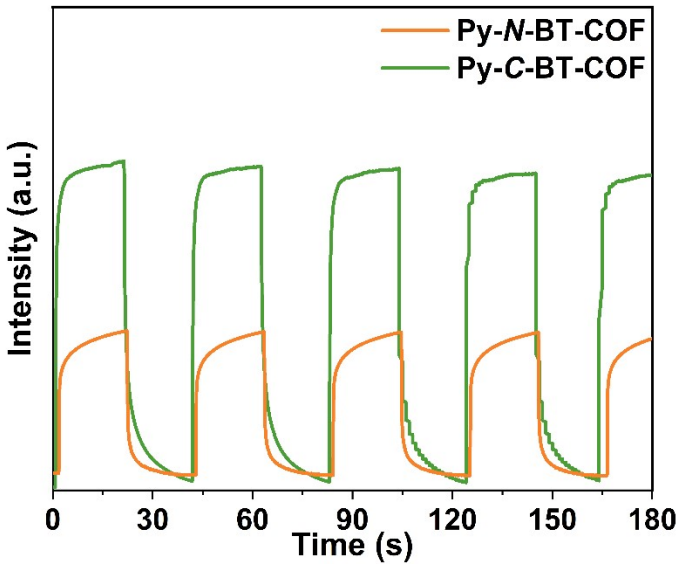

Figure S13. Transient photocurrent responses of Py-*C*-BT-COF (green) and Py-*N*-BT-COF (orange) under irradiation with ultraviolet/visible light.

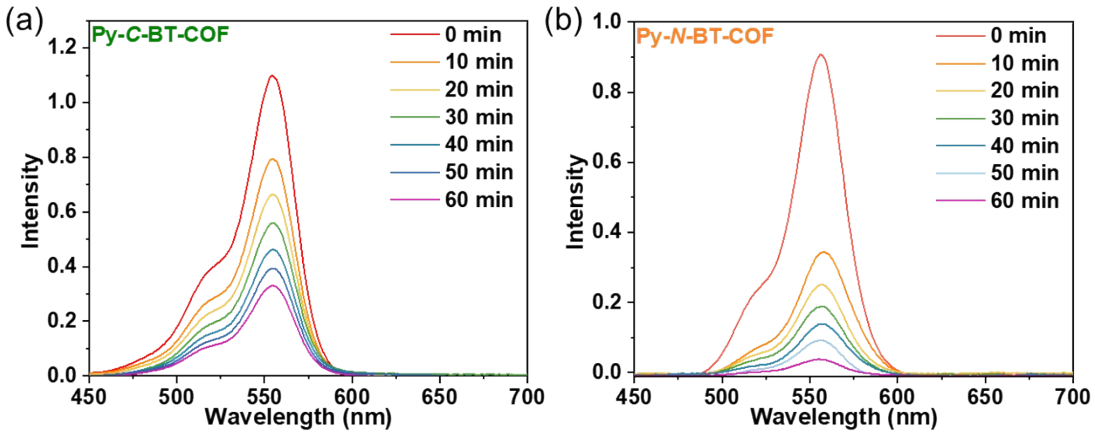

Figure S14. UV-vis spectra of rhodamine B (25 mg L^{-1}) after different illumination time intervals in the presence of Py-BT-COF isomers (0.5 mg mL^{-1}): (a) for Py-*C*-BT-COF and (b) for Py-*N*-BT-COF. (Optical source: 300 W xenon lamp with 420 nm optical filter).

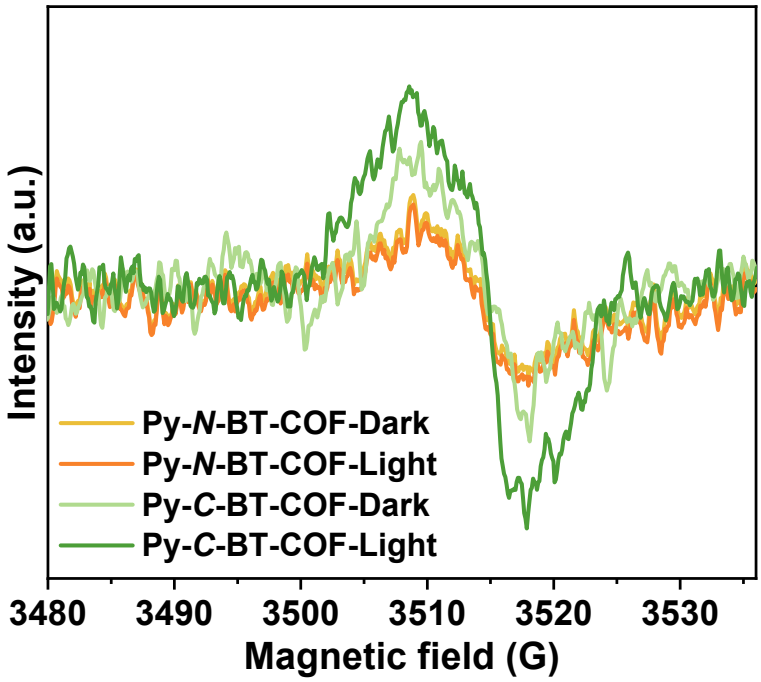

Figure S15. EPR spectra for Py-BT-COF isomers without trapping agent.

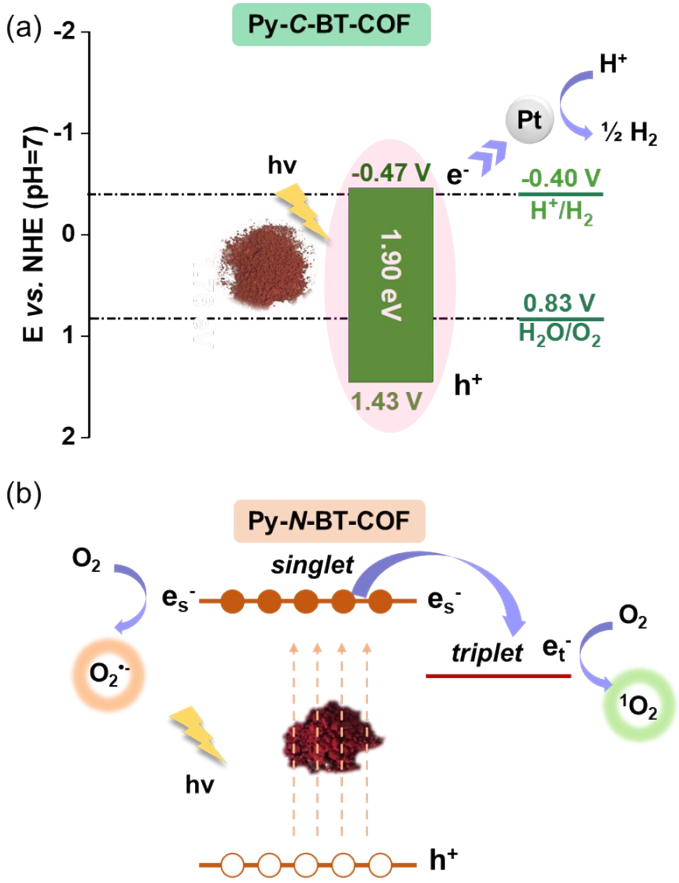

Figure S16. Proposed different photocatalytic transformation pathways for (a) Py-*C*-BT-COF and (b) Py-*N*-BT-COF, respectively.

Reference

1. Z. Li, T. Deng, S. Ma, Z. Zhang, G. Wu, J. Wang, Q. Li, H. Xia, S.-W. Yang and X. Liu, *J. Am. Chem. Soc.* **2023**, 145, 8364-8374.
2. T. Suzuki, T. Tsuji, T. Okubo, A. Okada, Y. Obana, T. Fukushima, T. Miyashi and Y. Yamashita, *J. Org. Chem*. **2001**, 66, 8954-8960.